

# Design and construction of kinetic structures based on elastica strips

Minghao Bi, Yunzhen He, Zhi Li, Ting-Uei Lee, Yi Min Xie\*

Centre for Innovative Structures and Materials, School of Engineering, RMIT University, Melbourne, Victoria 3001, Australia

## ARTICLE INFO

### Keywords:

Kinetic design  
Ruled surface  
Parametric modeling  
Elastica  
Lightweight construction

## ABSTRACT

Ruled surfaces have been used to create kinetic designs capable of reconfiguring their shapes to adapt to the environment and enhance aesthetic qualities. However, many existing designs require complex mechanical systems and heavy construction. Simplifying the design and construction process using an elastic-kinetic approach is promising but remains underexplored. This paper proposes a new strategy to rationalize kinetic designs with curved surfaces using a series of non-intersecting elastica strips bent to the minimum energy state. Complex 3D kinetic designs can be conveniently and parametrically modeled based on simple design parameters for 2D curves. The generated shapes are systematically classified into four categories. As a proof of concept, a full-scale kinetic pavilion was designed and constructed to demonstrate the effectiveness of the proposed method in realizing lightweight, high-speed, and cost-efficient construction. An extension of the proposed method to create interactive designs using sensors and actuators is also discussed.

## 1. Introduction

Ruled surfaces create elegant 3D forms by simply sweeping straight lines (rulings) along the path curves (directrices) [1,2]. This surface generation process has been widely adopted to create innovative and aesthetically striking structural forms [3,4]. Complex 3D surfaces created by straight rulings can be rationalized by a set of line segments, allowing smooth surfaces to be constructed using cost-effective elements [5]. When combined with hot-wire cutting [6], ruled surfaces can be fabricated by aligning the cutter in parallel with the straight rulings. Meanwhile, the shape and position of both rulings and directrices can be parametrically controlled, offering a wide variety of design options with few variables [7]. Favored by designers for their simplicity, ruled surfaces have seen applications in the design and construction of footbridge [8], pavilion [9], stone vault [10], shell structure [11], and buildings [4,12]. In pursuit of broader design potential, researchers have recently drawn their attention to developing new categories of ruled surfaces [13,14].

Elastica-ruled surfaces have been recently proposed based on the transformation of line-ruled surfaces [14]. Instead of using straight lines as rulings, elastically deformed curves are obtained from the analytical solution of a pinned-pinned elastica [15] and used as curved rulings. Sweeping all curved rulings creates a continuous elastica-ruled surface. By specifying the parameters of curved rulings, well-defined and elegant 3D surfaces can be conveniently obtained. Compared with line-ruled

surfaces, the extra geometrical freedom offered by curved rulings significantly adds variety to the design solutions. Furthermore, a rich set of cost-effective materials with elastic bending behavior can be used to realize elastica-ruled surfaces [16]. Existing studies on lined-ruled [1,2] and elastica-ruled surfaces [14] focus primarily on the design of static structures. Being fully parameterized, ruled surfaces' applications on kinetic designs show great potential but remain underexplored.

Kinetic architectural designs can reconfigure their shapes to achieve different objectives [17,18]. Apart from being aesthetically pleasing, such kinetic designs can be used on building envelopes and roofs to adjust sunlight and shading at different times of the day [19,20]. Combined with sensors, they can also transform into an intelligent and interactive design capable of actively responding to changing demands and environments [21]. However, the extra design freedom of kinetic designs comes together with increased complexity, resulting in mechanically complicated systems and heavy construction. For large-scale applications, kinetic structures are often segmented into small and repetitive modules to satisfy the construction constraints [19,22,23]. Assembly of such modules can be labor-intensive, time-consuming, and may require formwork to temporarily support the construction. Meanwhile, a large number of sensors and actuators are required to ensure the coordination of all kinetic modules, inflating the cost of design, construction, and maintenance [19,22]. As an alternative design strategy, elastic deformation has been used to create transformable structures through the bending and/or twisting of elastic lamellas, membranes,

\* Corresponding author.

E-mail address: [mike.xie@rmit.edu.au](mailto:mike.xie@rmit.edu.au) (Y.M. Xie).

strips, joints, deployable or developable surfaces [24–31]. The design strategy of using elastic deformation to achieve kinetic transformation is called an elastic kinetics approach. The mechanical systems in those designs are less complicated, and the generated energy can be stored and converted to electrical power [27]. The nonlinear elastic deformation and associated structural behavior induced by bending and twisting can be modeled using finite element analysis (FEA) [24–26,32].

Kinetic designs from ruled surfaces can be approximated by introducing movable directrices and discretized rulings. By continuously changing the shape of directrices, the dynamic transformation of rulings can create an attractive, kinetic visual effect, making it an effective strategy for creating kinetic architectural designs. The famous architect Santiago Calatrava has explored the potential of this strategy in designing sculptures [33,34], a pavilion [35], and a museum [36]. As a branch of the ruled surface family, elastica-ruled surfaces can be conveniently approximated without numerical discretization and constructed using lightweight elastic materials. In this regard, elastica-ruled surfaces have a vast potential for extension into kinetic designs with simple mechanical systems and cost-effective construction.

This paper proposes a new strategy for designing kinetic structures using moveable directrices and elastica strips. By continuously changing the shape or position of directrices, the kinetic transformation of complex curved surfaces can be rationalized through the elastic deformation of elastica strips. Depending on the motion behavior and characteristics of the directrices, the generated kinetic design can be systematically classified into four categories. The key features, requirements, and applications of each category are presented using 3D examples. As shown in Fig. 1, a full-scale kinetic pavilion is designed and constructed using the proposed method to demonstrate its capability to realize a lightweight, high-speed, and cost-effective construction. The pavilion can transform into a wide variety of geometrical forms through the simple radial motion of the inner directrix, and each form can be conveniently approximated using analytical solutions.

The novelty of the proposed design strategy is summarized as follows:

- The proposed strategy creates new possibilities for designing kinetic structures.
- Without needing FEA, the shape of the kinetic structure in each intermediate can be conveniently and accurately approximated using a simple analytical method.
- Based on an elastic-kinetic approach, structures created from the proposed method can be realized using simple mechanical systems.
- The effectiveness of the design strategy is demonstrated by a full-scale kinetic pavilion. Without needing formwork, its construction is lightweight, cost-effective, and high-speed.
- With a simple mechanism and lightweight construction, the proposed method shows great flexibility in being integrated with intelligent systems. By extension, it shows the potential to be transformed into interactive designs using sensors and actuators.

The remainder of the paper is organized as follows: Section 2 describes the numerical formulation of the proposed method. Section 3 shows the design and construction steps of a kinetic pavilion. Section 4

presents the construction results of the pavilion and the discussion. The conclusions are drawn in Section 5 to highlight the important features of the proposed design strategy.

## 2. Methodology

### 2.1. Ruled surfaces

In geometry, a surface is ruled if it is the union of a one-parameter family of straight lines, called its rulings [37]. A ruled surface can be described by the following parametric representation:

$$x(u, v) = a(u) + vr(u) \quad (1)$$

where  $a(u)$  is a path curve termed directrix, and  $r(u)$  is a vector field. For a fixed value of  $u_0$ , the expression  $x(u_0, v)$  represents the ruling or generator in the form of a straight line, pointing in the direction of  $r(u)$  (Fig. 2a). Geometrically speaking, a ruled surface is generated by continuously moving a line in space [2]. Each unique starting point on the directrix  $a(u)$  corresponds to another endpoint in the vector field, whose collection forms another directrix  $b(u)$ . Therefore, a ruled surface can also be described by the correspondence between two directrices  $a(u)$  and  $b(u)$  [38]:

$$x(u, v) = (1 - v)a(u) + vb(u) \quad (2)$$

The expression in eq. (2) requires each point on  $a(u)$  to map with a unique point on  $b(u)$ . The line connecting the two points becomes the ruling, which can be found as:

$$r(u) = b(u) - a(u) \quad (3)$$

Since both directrices are parametric curves, the shape of the generated ruled surface can be altered in two ways: (1) change the position and shape of any directrix; (2) change the mapping between directrices. Both methods affect the result by creating a new set of rulings. Fig. 2 illustrates how the change in mapping between directrices can lead to notably different ruled surfaces. While the position and shape of both directrices remain unaltered, the same start points in Fig. 2a now correspond to different endpoints in Fig. 2b. The change in the correspondence between directrices significantly affects the shape and

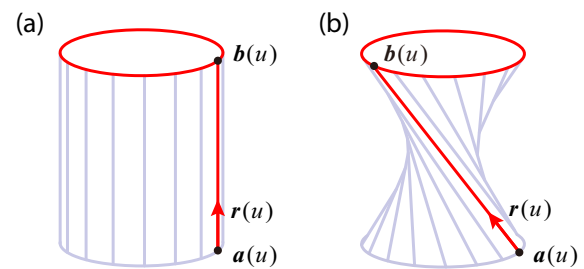


Fig. 2. Creating a ruled surface by sweeping a straight line along the directrices: (a) rulings are orientated vertically to create a cylindrical surface; (b) the change in mapping between directrices can significantly affect the generated ruled surface.



Fig. 1. Design and construction of a kinetic pavilion: (a) simulation of rulings and directrices using line frames (b) rendered result of the pavilion (c) picture of the assembled pavilion.

orientation of rulings, leading to a new ruled surface. By continuously varying the parameters of directrices, the transition of the ruled surfaces can generate a kinetic visual effect. For example, if the circular directrix  $b(u)$  in Fig. 2b is rotated around the central axis, the transformation of the ruled surface creates a ‘twist’ motion. This unique feature allows ruled surfaces to be used in designing kinetic structures.

In digital modeling, ruled surfaces gain popularity since complex 3D surfaces can be conveniently and parametrically controlled using simple curves. The simplicity of their numerical formulation allows them to be easily expanded into new design methods. The next subsections present how ruled surfaces can be combined with elastica curves into elastica-ruled surfaces.

### 2.2. Elastica curves

Elastica curves describe the naturally stable forms of a bent elastic strip [39], whose configuration has minimum bending energy and non-uniform curvature (Fig. 3a). Under different boundary conditions, elastica curves can be bent into various shapes. Such elastic deformations can be used to create novel bending active structures [40–42]. A unique feature of elastica curves is their material independency, meaning different materials can reach the same bent state using equivalent structural systems.

The numerical formulation of pinned-pinned elastica curves with a uniform bending stiffness is well studied in the literature [15]. Their mathematical expression is derived based on Jacobi elliptic functions using elliptic integrals, including the complete elliptic integral of the first kind  $K(m)$ , and the second kind  $E(m)$ . The value of  $m$  ranges from zero to one, and each  $m$  value corresponds to a unique bent state of an elastica curve.

Fig. 3b illustrates the shape of an elastica at different bent states. Each elastica curve can be characterized by four curve design parameters: the arc length  $L$ , the support distance  $b$ , the height of the curve after deformation  $h$ , and the initial tangent angle  $\Theta$ . The parametric representation of an elastica curve can be formulated based on the relationship between the  $m$  parameter and four curve design parameters:

$$\frac{b}{L} = 2 \frac{E(m)}{K(m)} - 1 \tag{4}$$

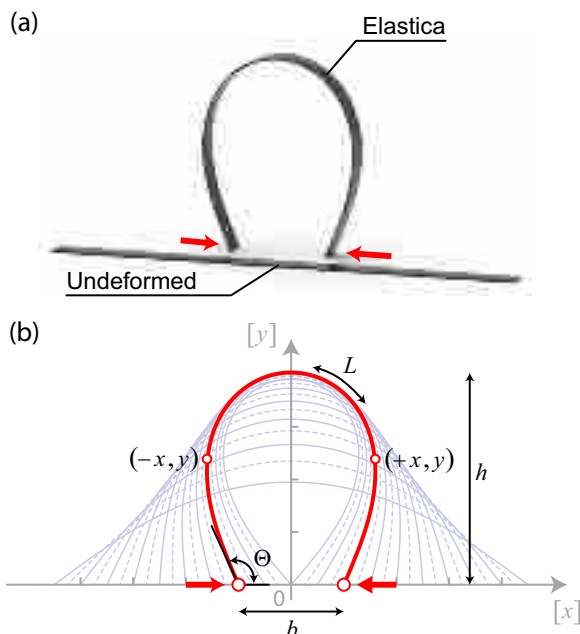


Fig. 3. Elastica curves: (a) a slender beam before and after bending; (b) parameters for determining the shape of an elastica curve.

$$\frac{h}{L} = \frac{\sqrt{m}}{K(m)} \tag{5}$$

$$\frac{b}{h} = \frac{2E(m) - K(m)}{m} \tag{6}$$

$$\Theta = 2\sin^{-1}(\sqrt{m}) \tag{7}$$

Based on the mathematical relationship, specifying any two design curve parameters gives the solutions for the other two unknowns. Hence, the designers can control the shape of an elastica curve using only two design curve parameters as variables. Once the design curve parameters are determined, they can be converted to  $(\pm x, y)$  coordinates in a cartesian system. Readers are referred to a previous paper for a detailed description of the mathematical formulation [14].

### 2.3. Elastica-ruled surfaces

Elastica-ruled surfaces are generated by transforming line-ruled surfaces using elastica curves as curved rulings. The resulting surface can be considered a subset of swept surfaces. The first step of the transformation process requires a line-ruled surface to be predetermined using directrices and rulings (Fig. 4a). As presented in Section 2.1, directrices can be created using parametric curves, and straight rulings are generated by connecting the corresponding points on the directrices. In the second step, elastica curves are generated based on the mathematical formulation in Section 2.2 and replace straight rulings. As shown in Fig. 4b, the value of the support distance  $b$  equals to the length of a straight ruling. Specifying an additional curve design parameter defines a unique elastica curve, which can be further rotated around the straight ruling by an angle  $\beta$  (Fig. 4b). Fig. 4c presents the elastica curves generated on all straight rulings, forming a complete set of curved rulings. By sweeping the curved rulings, a continuous elastica-ruled surface is constructed (Fig. 4d). As a straight line is the elastica in a relaxed state, line-ruled surfaces can be regarded as a special case of elastica-ruled surfaces.

The introduction of curved rulings creates a wide variety of design possibilities for elastica-ruled surfaces. Similar to line-ruled surfaces, the shape and position of the directrices can be parametrically controlled, allowing elastica-ruled surfaces to be extended into kinetic applications.

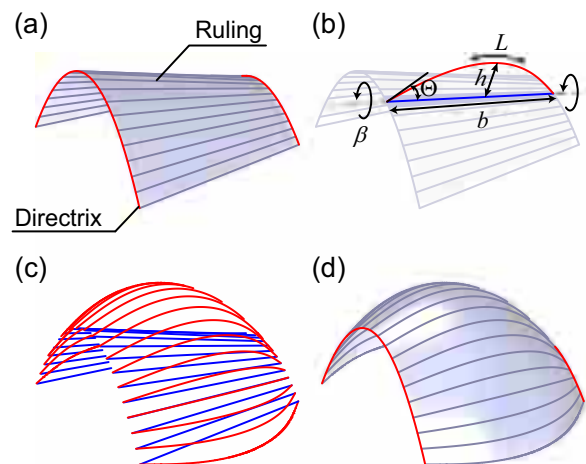


Fig. 4. Generation of an elastica-ruled surface: (a) a line-ruled surface; (b) generate an elastica curve on a straight ruling (c) curved rulings (red) and straight rulings (blue); (d) elastica-ruled surfaces. (For interpretation of the references to color in this figure, the reader is referred to the web version of this article.) (For interpretation of the references to color in this figure legend, the reader is referred to the web version of this article.)

2.4. Kinetic designs from elastica strips

Kinetic designs from elastica-ruled surfaces can be approximated using moveable directrices and elastica strips. By continuously changing the shape or position of directrices, the kinetic transformation of complex curved surfaces can be rationalized through the elastic deformation of elastica strips. Such kinetic designs can be reconfigured to different shapes to enhance aesthetic qualities and respond to environmental changes. Without requiring mechanically complex systems, this elastic-kinetic approach enables rapid geometrical transformation by simply changing the boundary conditions of the curved rulings. Designs in this paper use flexible elastica strip elements as rulings to approximate a continuous surface. In a practical application, the curved rulings can be constructed using elastic beam/strip elements, and a flexible membrane can be placed above the rulings to create a continuous surface.

For elastica with a pinned-pinned boundary, the shape of each curved ruling during kinetic transformation can be predicted using two curve design parameters (see Section 2.2). In most cases, rulings are realized through non-retractable elastica strips with a predetermined length, making the arc length  $L$  a fixed parameter. Therefore, one of the other three parameters— $b$ ,  $h$ , or  $\theta$ —must be varied continuously. Kinetic designs in this paper are generated based on the variation of the support distance  $b$ , which can be parametrically controlled by modifying the shape and position of the directrices. According to eq. (3), the change in the directrices  $\mathbf{a}(u)$  and  $\mathbf{b}(u)$  can create new straight rulings  $\mathbf{r}(u)$ . The length of the straight ruling  $|\mathbf{r}(u)|$  gives the value of support distance  $b$ . With  $L$  and  $b$  specified, the other two parameters— $h$  and  $\theta$ —can be calculated based on Eqs. (4) to (7). The parameter  $\beta$  controls the rotation of each curved ruling and provides an extra degree of design freedom. For the simplicity of the mechanical system, designs in this paper keep a consistent  $\beta$  for each curved ruling during kinetic movement. The shape and position of each curved ruling can be found based on the five parameters above. Finding all curved rulings defines the curved surface in each intermediate state during kinetic transformation.

2.4.1. Design workflow

The design workflow for the proposed strategy is presented in Fig. 5. Inputs of the algorithm include: (a) the collection of motions paths of two directrices  $A(t)$ ,  $B(t)$ ; (b) the time span of the motion,  $T$ ; (c) the number of curved rulings,  $N$ ; (d) the fixed arc length of each curved ruling,  $l_n$ ; (e) the fixed rotation angle of each curved ruling,  $\beta_n$ .

$A(t)$  and  $B(t)$  define the movement patterns of the two directrices as a function of time  $t$ . The shape and position of the two directrices at  $t_0$ — $\mathbf{a}(u)$  and  $\mathbf{b}(u)$ —can be found as  $A(t_0)$  and  $B(t_0)$ . Both directrices are divided into  $N$  points, forming pairs of boundary points ( $P_{a,n}$  and  $P_{b,n}$ ) to create curved rulings. Depending on the design, points can be equally or non-uniformly spaced along the directrices. For each pair of points, the support distance  $b_n$  is the linear distance between them,  $|P_{a,n}P_{b,n}|$ . Substituting  $b_n$  and  $l_n$  into Eqs. (4) to (7) gives the values of the other two curve design parameters,  $h_n$  and  $\Theta_n$ . With the additional rotation angle  $\beta_n$  specified by the designer, the shape of the curved ruling  $C_n$  can be defined. This process is repeated until all curved rulings are created to form the ruling set  $R_t$ . Combining the ruling sets in time sequence ( $R_{t_0}$ ,  $R_{t_1}$ , ...) generate the kinetic design  $S(t)$ .

Kinetic designs created using the design workflow in Fig. 5 can be further classified into four groups. The classification is based on the deformability of the directrix and the motion behavior of curved rulings, and both criteria can directly influence the level of design freedom and complexity. Fig. 6 summarises the key characteristics of each category of the kinetic designs. Details about their movement patterns are provided in the following subsections using examples.

The first criterion is related to the motions paths of the two directrices  $A(t)$ ,  $B(t)$ . A ‘rigid’ directrix remains unaltered in shape but changes its position during the transformation process (i.e.,  $A(t_0)$  and  $A(t_1)$  have the same shape but at different positions). In this system, the kinetic transformation of the structure is triggered by the motion of the entire rigid directrix (see Category 1 and 2 in Fig. 6). For a lightweight setup, only a single motion system is needed for each directrix, thus considerably lowering the overall complexity. In contrast, a directrix is ‘deformable’ if its shape changes during kinetic motion (i.e.,  $A(t_0)$  and  $A(t_1)$  have different shapes). For such a directrix, mechanical components

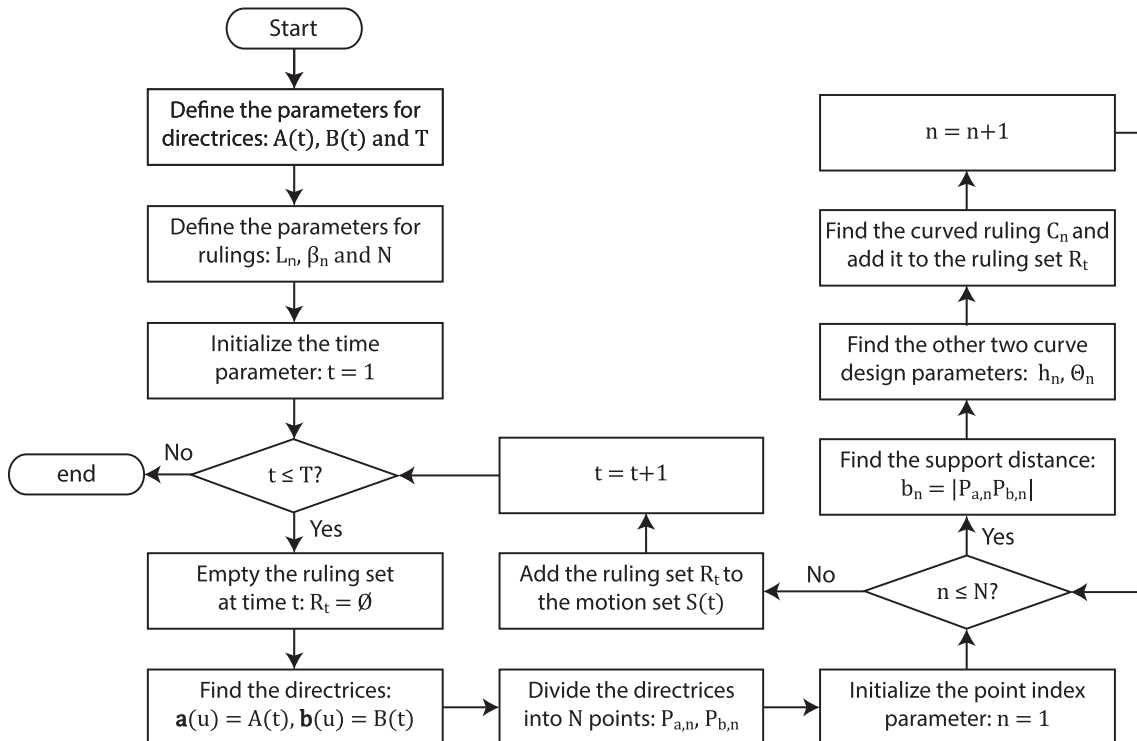


Fig. 5. The design workflow of the proposed method.

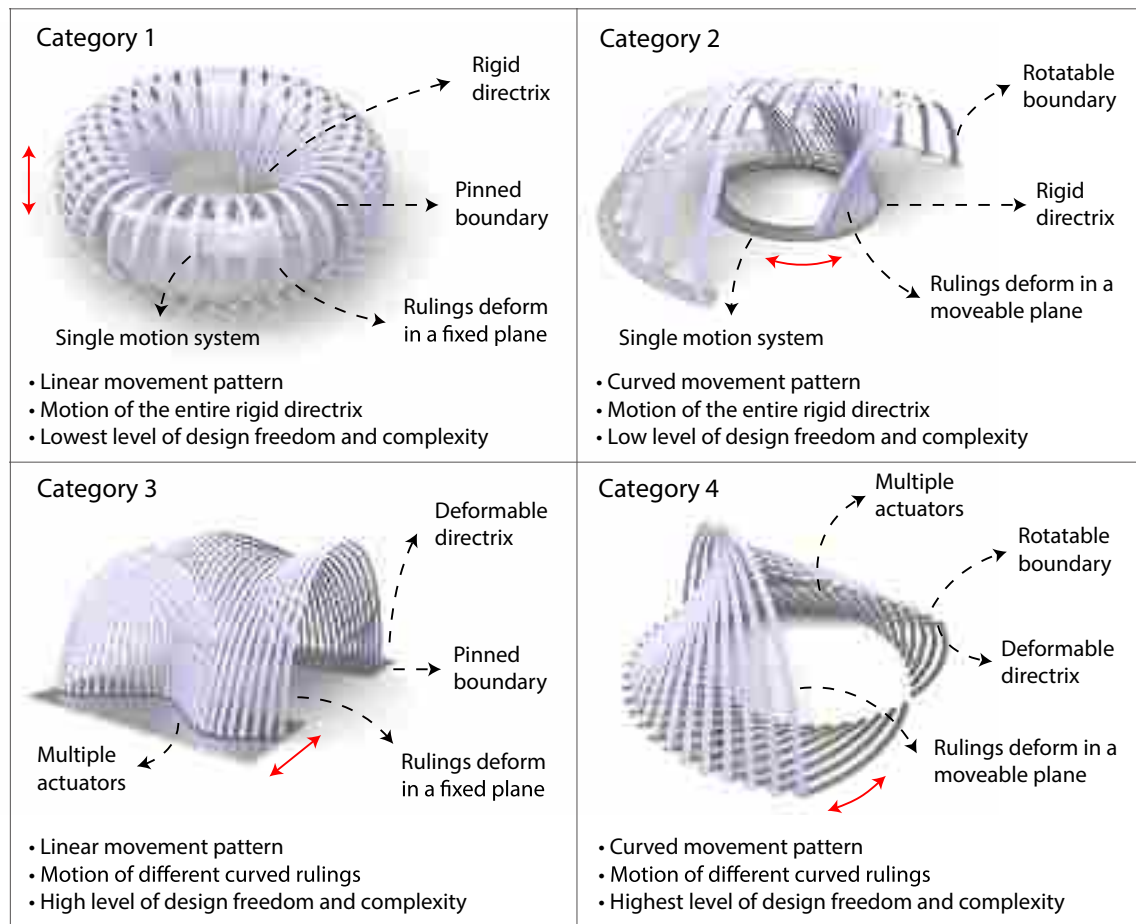


Fig. 6. Four design categories and their key features.

should be provided at the boundaries of each curved ruling to control their shape separately (see Category 3 and 4 in Fig. 6). While providing better design freedom, structures with a deformable directrix generally come at an increased cost and complexity.

The motion behavior of the curved rulings during kinetic movement is another criterion for classifying the designs. Eqs. (4) to (7) find the shape of a pinned-pinned elastica based on elastic deformation in a 2D plane without twisting. However, the motion path of curved rulings in a kinetic design may not remain in a fixed 2D plane. Consequently, elastica strips tend to twist during motion, making their shape hard to be predicted using simple analytical solutions. To prevent twisting, a rotatable component should be added to the boundaries of curved rulings to adjust the orientation of elastica strips. With a rotatable boundary condition, twisting will be automatically released as the elastica strips return to the minimum energy state. In summary, if the motion path of each curved ruling stays in the same 2D plane, there is no twisting effect in elastica strips, and only pinned-pinned boundary conditions are required (see Category 1 and 3 in Fig. 6). On the contrary, if the kinetic movement of curved rulings is generated in a moveable plane that creates curved movement patterns, rotatable frames should be provided for the boundaries to prevent twisting (see Category 2 and 4 in Fig. 6).

#### 2.4.2. Category 1: Rigid directrix with curved rulings deforming in a fixed plane

Designs in Category 1 have the lowest level of design freedom and complexity. With a rigid directrix and curved rulings deforming in a fixed plane, kinetic designs in this category do not require individual control of each curved ruling or rotatable frame on the boundaries. The kinetic design in Fig. 7a is created using two circular directrices and can

be scaled up to design the exterior surface of a stadium. The reconfiguration of the structure is triggered by moving the upper directrix in the vertical direction. Extensible columns can be created based on a telescopic mechanism to adjust the position of the upper directrix. By matching the center of both directrices, each curved ruling deforms in a consistent vertical plane during kinetic transformation. A lightweight, flexible membrane can be installed on top of the curved rulings to close the gaps between them. As the upper directrix changes its position, more sunlight can be allowed in the internal space.

#### 2.4.3. Category 2: Rigid directrix with curved rulings deforming in a moveable plane

With rotatable frames on the boundary, kinetic designs in Category 2 no longer require the elastic deformation of rulings to take place in a fixed 2D plane. As a result, curved motion patterns can be achieved through the movement of the rigid directrix. Fig. 7b illustrates a kinetic pavilion created by rotating a rigid directrix on a rail. In this design, the outer directrix is fixed in position while the inner directrix can be rotated around its center. The radial motion of the inner directrix can be achieved by combining a single motion system with a circular rail. The continuous variation of the support distance between directrices creates an aesthetically pleasing wave effect on the outer surface. With a rigid directrix controlled by a single mechanical system, the degree of design freedom and complexity is kept at a low level.

#### 2.4.4. Category 3: Deformable directrix with curved rulings deforming in a fixed plane

With a deformable directrix, designs in Category 3 are more flexible in geometry. The support distance of each curved ruling can be individually adjusted, giving designers more control over the structure's

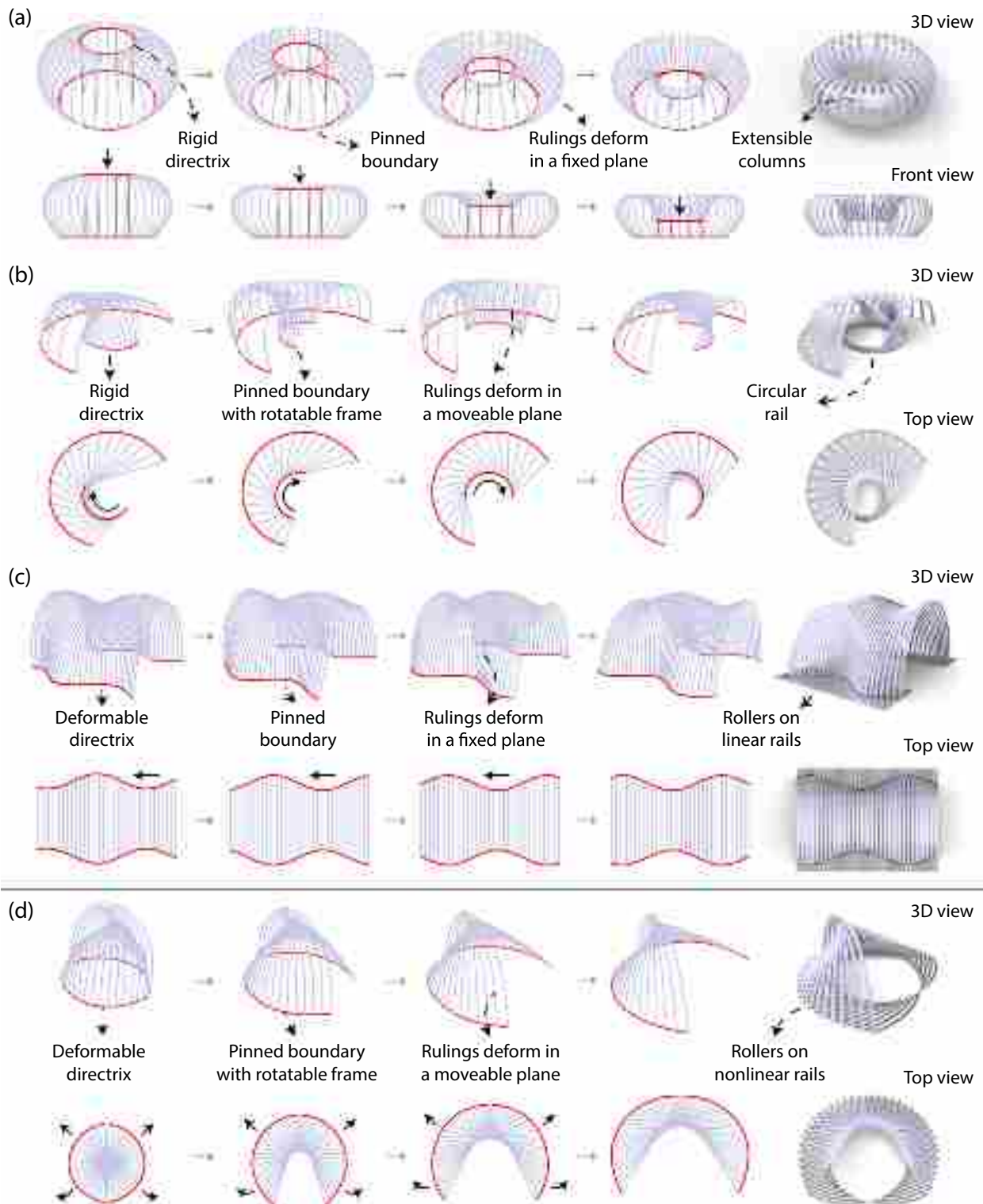


Fig. 7. Kinetic transformation of the designs in each category: (a) Category 1 (b) Category 2 (c) Category 3 (d) Category 4.

shape. However, the expanded design freedom is achieved at the price of increased mechanical complexity, as the boundary condition of each curved ruling needs to be controlled separately. Fig. 7c presents a kinetic tunnel design created using two deformable directrices. Curved rulings are placed in parallel, and rollers are placed at their ends to enable movement. In this example, the movement of the directrices is coordinated using a sine function, creating a parametrically controllable wave pattern on the surface. A wide variety of kinetic effects can be created by

programming the movement patterns of the directrices.

2.4.5. Category 4: Deformable directrix with curved rulings deforming in a moveable plane

With a deformable directrix and rotatable boundary frames, designs in Category 4 achieves the highest level of design freedom. Curved rulings no longer require a parallel setup, allowing more complex shapes and movement patterns to be realized. However, increased design

freedom is also associated with greater complexity due to nonlinear motion paths and the need for more boundary controls. Rotatable frames should be provided on the boundaries of the rulings to prevent twisting. Fig. 7d shows a kinetic dome design created from non-parallel curved rulings. As the directrices change in positions, the dome reconfigures from a closed state to an open state, allowing the internal space to be illuminated by sunlight. The lengths of the curved rulings are arranged in descending order to prevent them from interacting during the kinetic transformation. This interesting design can be placed on the ground as a pavilion or above a high-rise building as a transformable dome.

### 3. Case study: Nautilus pavilion

To demonstrate the potential applications of the proposed strategy, a full-scale kinetic pavilion is designed and constructed based on the numerical model presented in Fig. 7b. This section presents the design details and construction steps of the kinetic pavilion.

The kinetic pavilion design in Fig. 7b is created using three main components: a fixed outer directrix with a spiral shape, a moveable inner directrix with a circular shape, and 20 curved rulings between them. With a relatively simple mechanical system, the kinetic transformation of the structure can be triggered by the radial motion of the rigid inner directrix. In this design, curved rulings deform in a moveable plane, thereby requiring rotatable frames on the boundaries to prevent elastica strips from twisting. Connection details and the mechanical system should be carefully designed to achieve the desired outcome.

The name of the design—nautilus pavilion—is inspired by its shape in the top view, which resembles the cross-section of a nautilus seashell. As shown in Fig. 8, the overall dimension of the pavilion is 6 m × 6.2 m. The inner directrix is designed using a ring-shaped turntable, whose inner and outer diameters are 0.9 m and 2.6 m, respectively. With a spiral outer boundary, the pavilion has a minimum internal width of 1.2 m at one end and a maximum of 2.2 m at the other. With 5 m long elastica strips as curved rulings, the internal space of the pavilion is designed to allow human passage.

Fig. 9 illustrates the details of the kinetic pavilion design. For easy transportation and assembly, the inner and outer directrices are partitioned into segments and designed with an interlocking mechanism. All segments are produced from medium-density fibreboard (MDF) using a CNC machine.

The radial motion of the inner directrix is achieved by a turntable made of three layers: a circular MDF base (bottom), a metal moving track (middle), and an MDF loading platform (top). The base layer and the loading platform are cut in quarters and can be assembled manually

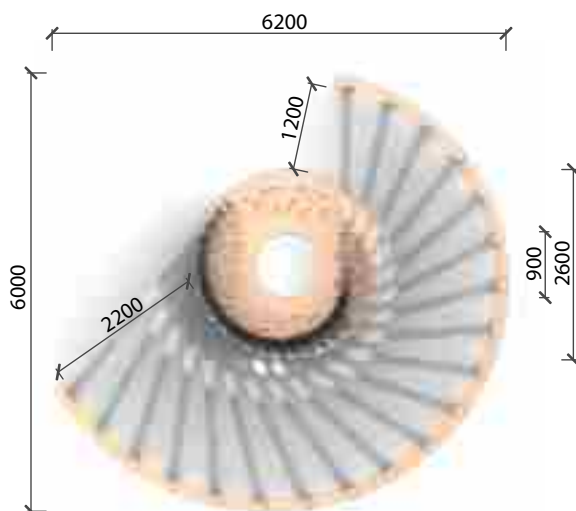


Fig. 8. Dimensions of the kinetic pavilion design in the top view.

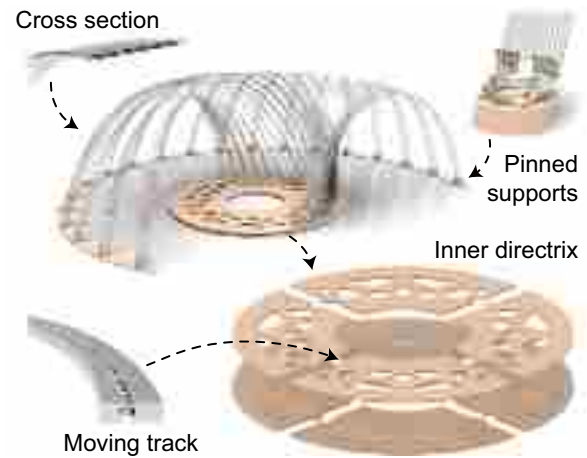


Fig. 9. Components of the proposed pavilion design, including polycarbonate elastica strips, metal support frames, metal moving track, and MDF bases and turntable.

by matching the interlocking shapes. To reduce the weight and improve the aesthetic quality, the loading platform is topology optimized using the bi-directional evolutionary structural optimization method [43]. When combined with additive or subtractive manufacturing techniques, this topology optimization method can increase structural efficiency and lower the weight [44–46]. The resulting shape has an organic geometry and achieves a 40% weight reduction compared to a solid plate. In contrast, the base has a solid cross-section to provide weight and stability to the entire body. In the middle layer, the moving track consists of a series of metal balls sandwiched by two metal tracks, enabling their relative rotation with little friction. The bottom surface of the outer track is connected to the base, while the upper surface of the inner track is joined to the loading platform. In addition, eight roller wheels are placed near the edge of the base to further support the loading platform. With the help of the metal tracks and roller wheels, the loading platform can be easily and smoothly rotated without changing its position. Together, the assembled turntable has a 2.6 m diameter and 60 mm thickness. With a lightweight setup, the rotation of the turntable can be controlled manually. A motor system can be introduced to control the rotation in the future to realize automatic kinetic transformation.

The outer boundary (representing the outer directrix) is designed as a spiral MDF strip and is divided into ten modules. With a dimension of approximately 1.2 m × 0.2 m, all modules are nested in a 3 m × 1.3 m rectangular region and are produced using a single plate to minimize material waste. To ensure endpoints of curved rulings are on the same level, small cylindrical bases made of MDF are installed on the outer boundary to match the height of the turntable. With a solid cross-section, the outer boundary has sufficient weight to remain in its position while other components are moving.

Twenty curved rulings in this design are realized using polycarbonate elastica strips with a dimension of 5000 mm × 140 mm × 10 mm. With a hollow section strengthened by structural ribs, the elastica strips have an increased second moment of inertia and reduced weight. Light strips can also be placed within the hollow section to create a light effect for the pavilion at night. With a flexible behavior, each strip can be rolled into a circle with a 1.5 m diameter for easy transportation and storage.

Fig. 10 compares the simulated elastica curve profile with the elastica strip bent to different intermediate states. The comparison aims to examine the bending behavior of the manufactured elastica, which is sensitive to the actual boundary condition and material properties. The support distance  $b$  is continuously varied from 3550 mm to 1050 mm, covering the deformation range of the curved rulings in this design. The ratio between the support distance  $b$  and arc length  $L$  is used to describe

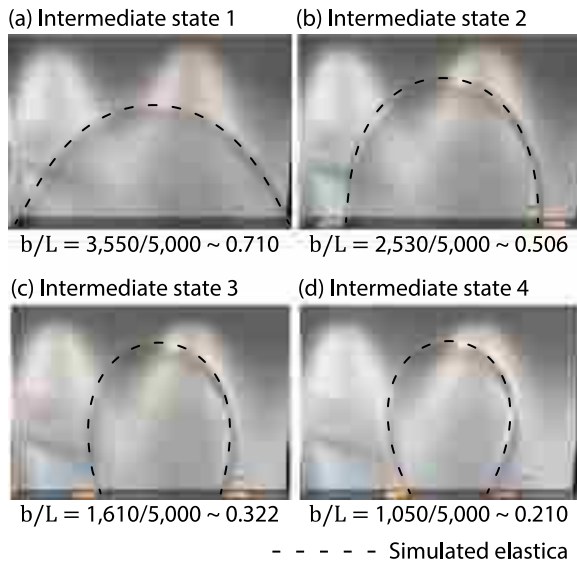


**Fig. 10.** Comparison of the simulated elastica curve profile (black dotted curves) against the bent polycarbonate strip (photos in the background) in different intermediate states. The support distance  $b$  is measured to generate analytical solutions for the 5-m-long elastica strip. (For interpretation of the references to color in this figure, the reader is referred to the web version of this article.)

the bent state, which ranges from 0.710 to 0.210. For the analytical solution, the measured values of  $b$  and  $L$  are used to calculate the other two curve design parameters, as summarized in Table 1. Compared to the simulated result, the physical structure has a slightly lower height after deformation  $h$  and a higher initial tangent angle  $\Theta$ , but the largest difference is below 4%. The match between the simulated and constructed results suggests that the theoretical elastica assumptions have been preserved in the current setup. After releasing the boundaries, the strip can restore to the flat state without being permanently deformed, indicating that the tested deformation is within the elastic range.

Pinned supports with rotatable frames are used to connect the elastica strips with the boundaries, as shown in Fig. 9. A small metal turntable enables the rotation of the support to prevent the elastica strips from twisting. On top of it, two pairs of brackets and hinges are combined to create a pinned connection. Different components are connected via bolts and nuts. The simplicity of the connection design allows all components to be easily assembled and disassembled.

Fig. 11 illustrates the main steps for assembling the nautilus pavilion. Firstly, the MDF base and turntable were manufactured using CNC cutting, and metal support components were installed at the ends of the elastica strips. Subsequently, MDF components were joined by matching the interlocking shapes, and the moving track was placed between the base and turntable to enable rotation. Finally, 20 elastica strips were sequentially assembled by joining their support frames to the inner turntable and outer boundary. With lightweight materials and simple mechanical setups, the entire onsite assembly was finished within half a

**Table 1**

Comparison of the curve design parameters between the physical bent strip and the simulated elastica curve. For the analytical solution, the measured values of support distance  $b$  and arc length  $L$  are used to calculate the other two curve design parameters.

Curve design parameters	Comparison category	Intermediate state 1	Intermediate state 2	Intermediate state 3	Intermediate state 4
Support distance $b$ (mm)	Physical test	5000	5000	5000	5000
	Simulation	same	same	same	same
Arc length $L$ (mm)	Physical test	3550	2530	1610	1050
	Simulation	same	same	same	same
Height after deformation $h$ (mm)	Physical test	1540	1840	1940	1970
	Simulation	1550	1860	1990	2020
Initial tangent angle $\Theta$ (°)	Physical test	65.9	88.5	103.7	114.2
	Simulation	63.7	85.2	102.4	112.5

day by three people. The structure can also be easily disassembled, transported, and reused for future applications. A video file is provided to show the construction process and results of the kinetic pavilion.

## 4. Results and discussion

### 4.1. Comparison between simulated and constructed results

Fig. 12 compares the simulated and constructed results when the inner directrix of the pavilion is rotated at different angles. With a decreasing support distance from Fig. 12a to Fig. 12d, the height of the kinetic pavilion gradually increases. Further rotation of the MDF turntable relocates the pavilion's entrance to the right side and lowers its height. With rotatable support frames, the polycarbonate strips deform elastically in a vertical plane without twisting or interacting with each other. Overall, the elastic deformations of the strips match well with the simulations, confirming that complex kinetic designs can be conveniently and inexpensively achieved using the proposed strategy. From a visual comparison, the slight mismatch between the simulated and constructed results can be attributed to a few reasons. (1) Uneven ground and manual assembly can create construction errors; (2) The metal supports may not fully preserve the theoretical assumptions of pinned-pinned boundary; (3) Strong winds can create unpredictable external forces on the structures and affect the shape of the elastica strips; (4) There is a slight discrepancy in the camera angle and position between the two results.

When viewed from outside the structure, the kinetic movement of the pavilion generates visually stunning effects. Users can rotate the turntable inside the structure to change the "shape" of their surroundings. As the polycarbonate strips are transparent, walking inside the pavilion feels like being protected by a barrel wave. With LED lights on at night, the pavilion turns into an array of evolving light strips and becomes more aesthetically pleasing (Fig. 13).

### 4.2. Potential extension

The current pavilion design can be further improved by installing motors and sensors to transform it into an interactive structure. Instead of manually rotating the turntable, it can be digitally controlled based on current environmental conditions and immediate user-specified commands. The gap between curved rulings can be covered using a flexible membrane to protect users from sunlight and wind. The properties of the selected membrane, including size, shape, material, and connection methods, need to be carefully designed and tested to prevent overstretching and achieve the desired outcome during kinetic transformation. By extension, the pavilion can adjust its orientation based on environmental data collected by sensors to increase the level of comfort. For this pavilion design, the rotation of the structure can also be programmed to follow human movements. As a person walks through the inner space, the directrix can be automatically adjusted to center the viewer inside the pavilion. From the viewer's viewpoint, the arches ahead open up, whereas the ones behind close up.

This paper predicts elastic deformation using analytical solutions for



Fig. 11. The construction steps of the nautilus pavilion: (1) MDF components were produced using CNC machining; (2) support frames were assembled and connected to elastica strips; (3) MDF bases were placed onsite in the correct position; (4) the moving track was installed on the inner base; (5) the turntable was connected to the moving track; (6) elastica strips were joined to the inner turntable and outer boundary.

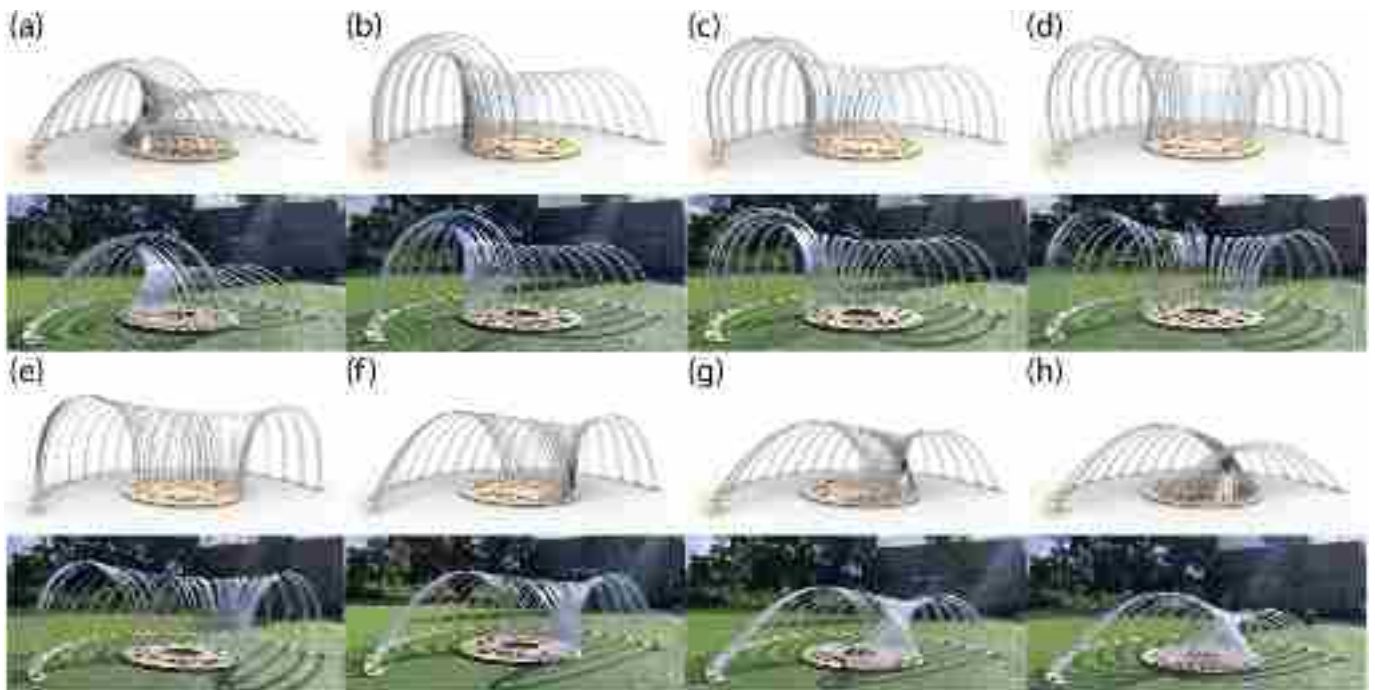


Fig. 12. The comparison between the simulated 3D model (top) and constructed kinetic pavilion (bottom) in eight different states. With state (a) as the starting point, the MDF turntable has been rotated in the clockwise direction by various angles: (b) 60°; (c) 90°; (d) 130°; (e) 175°; (f) 220°; (g) 250°; (h) 280°.



Fig. 13. A comparison of the kinetic pavilion in the daytime and at night.

a pinned-pinned elastica. Under different boundary conditions, a wide range of other solutions exist, which can be predicted using physical models or numerical methods. By extension, the support frames of the curved rulings can be extended from pinned to fixed or partially fixed conditions, thereby adding more variety to design solutions. The arc length  $L$  and rotation parameter  $\beta$  can also be changed from fixed to variable design parameters to explore more design possibilities. Because of the simplicity of the proposed design strategy, those further extensions can be easily implemented by modifying the boundary conditions of the structure.

The proposed design strategy can be used to create kinetic architectural designs for different objectives. Other potential architectural applications include: (1) kinetic components on a building façade to adjust ventilation and interior light; (2) creating dynamic patterns on a media façade; (3) reconfigurable dome with open and close states; (4) transformable structural skeleton to support flexible membrane; (5) Kinetic landmark sculptures.

## 5. Conclusion

This paper proposes a novel design strategy to create kinetic structures using an elastic-kinetic approach. By continuously changing the shape or position of directrices, kinetic designs with curved surfaces can be rationalized using a series of non-intersecting elastica strips bent to the minimum energy state. Complex 3D kinetic designs can be conveniently and parametrically modeled based on simple parameters that control the bent states of 2D curves. In each intermediate state during kinetic transformation, the shape of curved rulings can be determined based on the support distance between directrices and the fixed length of elastica strips. Continuously varying the support distance using moveable directrices can generate a kinetic motion pattern on the strips' surface to achieve striking visual effects.

Designs created using the proposed strategy are classified into four categories based on the characteristics of the directrices and curved rulings. A rigid directrix remains unaltered in shape, and its movement patterns can be triggered by translation or rotation using a simple mechanical system. In contrast, designs with a deformable directrix allow the shape of curved rulings to be individually controlled, leading to an increased level of flexibility and complexity. If curved rulings deform in a fixed 2D plane, the elastica profile can be achieved using simple pinned-pinned supports. Contrarily, designs with curved rulings

deforming in a moveable plane require rotatable frames at the boundaries to prevent elastica strips from twisting. Examples in each category demonstrate their key features, requirements, and potential applications in kinetic architecture.

As a proof of concept, a full-scale kinetic pavilion was designed and built to demonstrate the effectiveness of the proposed method in realizing lightweight, high-speed, and cost-efficient construction. The constructed pavilion is compared against the simulated result when the inner directrix is rotated at eight different angles. As shown in the provided video file, the kinetic movement of the pavilion can generate visually stunning effects. With LED lights switched on at night, the pavilion turns into an array of evolving light strips and becomes more aesthetically pleasing. The concept and findings presented in this paper create new possibilities in kinetic architectural design.

In future works, structures created using the proposed strategy can be further extended into interactive designs using sensors and actuators. Depending on the applications, a wide variety of elastic materials and geometrical configurations can be used to explore different design possibilities.

Supplementary data to this article can be found online at <https://doi.org/10.1016/j.autcon.2022.104659>.

## Replication of results

Data and code availability: The code for this work is available from the corresponding author upon reasonable request.

## Declaration of Competing Interest

The authors declare that they have no known competing financial interests or personal relationships that could have appeared to influence the work reported in this paper.

## Data availability

Data will be made available on request.

## Acknowledgment

This project was supported by the Australian Research Council (FL190100014, DP200102190).

## References

- [1] H. Pottmann, W. Lü, B. Ravani, Rational ruled surfaces and their offsets, *Graphical Models Image Process.* 58 (6) (1996) 544–552, <https://doi.org/10.1006/gmp.1996.0045>.
- [2] M. Peternell, H. Pottmann, B. Ravani, On the computational geometry of ruled surfaces, *Comput. Aided Des.* 31 (1) (1999) 17–32, [https://doi.org/10.1016/S0010-4485\(98\)00077-3](https://doi.org/10.1016/S0010-4485(98)00077-3).
- [3] G. Glaeser, F. Gruber, Developable surfaces in contemporary architecture, *J. Math. Arts.* 1 (1) (2007) 59–71, <https://doi.org/10.1080/17513470701230004>.
- [4] I.A. Mamieva, Influence of the geometrical researches of ruled surfaces on design of unique structures, *Struct. Mech. Eng. Construct. Build.* 15 (4) (2019) 299–307, <https://doi.org/10.22363/1815-5235-2019-15-4-299-307>.
- [5] M.I. Gómez Sánchez, A. González Uriel, I. García Ríos, Ruled surfaces and parametric design, in: C.L. Marcos (Ed.), *Graphic Imprints*, Springer International Publishing, Cham, 2019, pp. 231–241, [https://doi.org/10.1007/978-3-319-93749-6\\_19](https://doi.org/10.1007/978-3-319-93749-6_19).
- [6] B. van Sosin, M. Bartoň, G. Elber, Accessibility for line-cutting in freeform surfaces, *Comput. Aided Des.* 114 (2019) 202–214, <https://doi.org/10.1016/j.cad.2019.05.014>.
- [7] E. Prousalidou, S. Hanna, A parametric representation of ruled surfaces, in: A. Dong, A. Vande Moere, J.S. Gero (Eds.), *Computer-Aided Architectural Design Futures (CAADFutures) 2007*, Springer Netherlands, Dordrecht, 2007, pp. 265–278, [https://doi.org/10.1007/978-1-4020-6528-6\\_20](https://doi.org/10.1007/978-1-4020-6528-6_20).
- [8] K. Noack, D. Lordick, Optimized ruled surfaces with an application to thin-walled concrete shells, in: L. Cocchiarella (Ed.), *ICGG 2018 - Proceedings of the 18th International Conference on Geometry and Graphics*, Springer International Publishing, Cham, 2019, pp. 338–349, [https://doi.org/10.1007/978-3-319-95588-9\\_27](https://doi.org/10.1007/978-3-319-95588-9_27).

- [9] A. Martín-Pastor, R. García-Alvarado, Developable wooden surfaces for lightweight architecture: Bio-dune pavilion, in: F. Bianconi, M. Filippucci (Eds.), *Digital Wood Design: Innovative Techniques of Representation in Architectural Design*, Springer International Publishing, Cham, 2019, pp. 1481–1500, [https://doi.org/10.1007/978-3-030-03676-8\\_60](https://doi.org/10.1007/978-3-030-03676-8_60).
- [10] M. Rippmann, P. Block, New design and fabrication methods for freeform stone vaults based on ruled surfaces, in: C. Gengnagel, A. Kilian, N. Palz, F. Scheurer (Eds.), *Computational Design Modelling*, Springer, Berlin, Heidelberg, 2012, pp. 181–189, [https://doi.org/10.1007/978-3-642-23435-4\\_21](https://doi.org/10.1007/978-3-642-23435-4_21).
- [11] B. Postle, Methods for creating curved shell structures from sheet materials, *Buildings*. 2 (4) (2012) 424–455, <https://doi.org/10.3390/buildings2040424>.
- [12] G. Gui, The ruled surface nature of hyperbolic paraboloid and its applications, *Manag. Sci. Eng.* 14 (2) (2020) 1–4, <https://doi.org/10.3968/11965>.
- [13] V. Nikolić, O. Nikolić, J. Tamburić, S.S. orđević, S. Janković, Higher-order ruled surfaces and their possible use in architectural design, *Nexus Network Journal* 21 (1) (2019) 129–147, <https://doi.org/10.1007/s00004-018-00425-0>.
- [14] T.-U. Lee, Y.M. Xie, From ruled surfaces to elastica-ruled surfaces: new possibilities for creating architectural forms, *J. Int. Assoc. Shell Spatial Struct.* 62 (4) (2021) 271–281, <https://doi.org/10.20898/j.iaass.2021.014>.
- [15] A. Valiente, An experiment in nonlinear beam theory, *Am. J. Phys.* 72 (8) (2004) 1008–1012, <https://doi.org/10.1119/1.1738427>.
- [16] T.-U. Lee, X. Yang, J. Ma, Y. Chen, J.M. Gattas, Elastic buckling shape control of thin-walled cylinder using pre-embedded curved-crease origami patterns, *Int. J. Mech. Sci.* 151 (2019) 322–330, <https://doi.org/10.1016/j.ijmecsci.2018.11.005>.
- [17] T.V. Belyaeva, Dynamic architecture. Interaction with city, nature, man, in: IOP Conference Series: Materials Science and Engineering 687 (5), 2019, p. 55015, <https://doi.org/10.1088/1757-899X/687/5/055015>.
- [18] Y.V. Gorgorova, M.G. Sarkisyan, Dynamic architecture as reflection of a modern information society, *Mater. Sci. Forum* 931 (2018) 699–704, <https://doi.org/10.4028/www.scientific.net/MSF.931.699>.
- [19] M. Barozzi, J. Lienhard, A. Zanelli, C. Monticelli, The sustainability of adaptive envelopes: developments of kinetic architecture, *Proc. Eng.* 155 (2016) 275–284, <https://doi.org/10.1016/j.proeng.2016.08.029>.
- [20] M. Asefi, Transformation and movement in architecture: the marriage among art, engineering and technology, *Procedia Soc. Behav. Sci.* 51 (2012) 1005–1010, <https://doi.org/10.1016/j.sbspro.2012.08.278>.
- [21] W.M. Kroner, An intelligent and responsive architecture, *Autom. Constr.* 6 (5) (1997) 381–393, [https://doi.org/10.1016/S0926-5805\(97\)00017-4](https://doi.org/10.1016/S0926-5805(97)00017-4).
- [22] S. Attia, Evaluation of adaptive facades: the case study of Al Bahr towers in the UAE, *QScience Connect*. 2 (2017) 6, <https://doi.org/10.5339/connect.2017.qgbc.6>.
- [23] G. Grunwald, T. Hermeking, T. Prang, Kinetic roof structure: Msheireb heart of Doha, *Proc. Eng.* 155 (2016) 289–296, <https://doi.org/10.1016/j.proeng.2016.08.031>.
- [24] J. Lienhard, S. Schleicher, S. Poppinga, T. Masselter, M. Milwich, T. Speck, J. Knippers, Flectofin: a hingeless flapping mechanism inspired by nature, *Bioinspir. Biomimetics* 6 (4) (2011) 45001–45007, <https://doi.org/10.1088/1748-3182/6/4/045001>.
- [25] S. Brancart, L. De Laet, N. De Temmerman, Deployable textile hybrid structures: design and modelling of kinetic membrane-restrained bending-active structures, *Proc. Eng.* 155 (2016) 195–204, <https://doi.org/10.1016/j.proeng.2016.08.020>.
- [26] J. Lienhard, J. Knippers, Considerations on the scaling of bending-active structures, *Int. J. Space Struct.* 28 (3–4) (2013) 137–148, <https://doi.org/10.1260/0266-3511.28.3-4.137>.
- [27] J. Knippers, T. Speck, Design and construction principles in nature and architecture, *Bioinspir. Biomimetics* 7 (2012) 15002, <https://doi.org/10.1088/1748-3182/7/1/015002>.
- [28] T.-U. Lee, J.M. Gattas, Y.M. Xie, Bending-active kirigami, *Int. J. Solids Struct.* 254–255 (2022), 111864, <https://doi.org/10.1016/j.ijsolstr.2022.111864>.
- [29] P. Sareh, The least symmetric crystallographic derivative of the developable double corrugation surface: computational design using underlying conic and cubic curves, *Mater. Des.* 183 (2019), 108128, <https://doi.org/10.1016/j.matdes.2019.108128>.
- [30] E. Schling, J. Schikore, Morphology of kinetic asymptotic grids, in: C. Gengnagel, O. Baverel, G. Betti, M. Popescu, M.R. Thomsen, J. Wurm (Eds.), *Towards Radical Regeneration: Design Modelling Symposium Berlin 2022*, Springer Nature, Cham, 2022, pp. 374–393, [https://doi.org/10.1007/978-3-031-13249-0\\_31](https://doi.org/10.1007/978-3-031-13249-0_31).
- [31] E. Schling, D. Hitec, R. Barthel, Designing grid structures using asymptotic curve networks, in: K. De Rycke, C. Gengnagel, O. Baverel, J. Burry, C. Mueller, M. M. Nguyen, P. Rahm, M.R. Thomsen (Eds.), *Humanizing Digital Reality: Design Modelling Symposium Paris 2017*, Springer Singapore, Singapore, 2018, pp. 125–140, [https://doi.org/10.1007/978-981-10-6611-5\\_12](https://doi.org/10.1007/978-981-10-6611-5_12).
- [32] A.-K. Goldbach, A.M. Bauer, R. Wüchner, K.-U. Bletzinger, CAD-integrated parametric lightweight design with isogeometric B-rep analysis, *Front. Built Environ.* 6 (2020) 44, <https://doi.org/10.3389/fbuil.2020.00044>.
- [33] S. Calatrava, Shadow machine. <https://calatrava.com/motion/shadow-machine-new-york.html>, 1993 (accessed July 21, 2022).
- [34] S. Calatrava, SMU Meadows Museum Wave Sculpture. <https://calatrava.com/projects/smu-meadows-museum-wave-sculpture-dallas.html>, 2002.
- [35] S. Calatrava, Kuwait Pavilion. <https://calatrava.com/projects/kuwait-pavilion-sev-illa.html>, 1992 (accessed July 21, 2022).
- [36] S. Calatrava, Milwaukee Art Museum (MAM). <https://calatrava.com/projects/milwaukee-art-museum.html>, 2001 (accessed April 30, 2022).
- [37] M. Berger, B. Gostiaux, *Differential Geometry: Manifolds, Curves, and Surfaces*, 1st ed., Springer, New York, New York, 1988 <https://doi.org/10.1007/978-1-4612-1033-7>. ISBN 978-1-4612-1033-7.
- [38] C. Tang, P. Bo, J. Wallner, H. Pottmann, Interactive design of developable surfaces, *ACM Trans. Graph.* 35 (2) (2016) 1–12, <https://doi.org/10.1145/2832906>.
- [39] L. Euler, *Methodus Inveniendi Lineas Curvas Maximi Minimive Proprietate Gaudentes Sive Solutio Problematis Isoperimetrici Latissimo Sensu Accepti*, Birkhäuser Basel, 1744 (ISBN 978-3-7643-1424-8.).
- [40] Y. Sakai, M. Ohsaki, Discrete elastica for shape design of gridshells, *Eng. Struct.* 169 (2018) 55–67, <https://doi.org/10.1016/j.engstruct.2018.05.002>.
- [41] B. D'Amico, A. Kermani, H. Zhang, A. Pugnale, S. Colabella, S. Pone, Timber gridshells: numerical simulation, design and construction of a full scale structure, *Structures*. 3 (2015) 227–235, <https://doi.org/10.1016/j.istruc.2015.05.002>.
- [42] W. Huang, C. Wu, J. Hu, W. Gao, Weaving structure: a bending-active gridshell for freeform fabrication, *Autom. Constr.* 136 (2022), 104184, <https://doi.org/10.1016/j.autcon.2022.104184>.
- [43] X. Huang, Y.M. Xie, *Evolutionary Topology Optimization of Continuum Structures: Methods and Applications*, John Wiley & Sons, Ltd, Chichester, England, 2010, <https://doi.org/10.1002/9780470689486>. ISBN 9780470689486.
- [44] M. Bi, L. Xia, P. Tran, Z. Li, Q. Wan, L. Wang, W. Shen, G. Ma, Y.M. Xie, Continuous contour-zigzag hybrid toolpath for large format additive manufacturing, *Additive Manuf.* 55 (2022), 102822, <https://doi.org/10.1016/j.addma.2022.102822>.
- [45] M. Bi, P. Tran, Y.M. Xie, Topology optimization of 3D continuum structures under geometric self-supporting constraint, *Additive Manuf.* 36 (2020), 101422, <https://doi.org/10.1016/j.addma.2020.101422>.
- [46] M. Bi, P. Tran, L. Xia, G. Ma, Y.M. Xie, Topology optimization for 3D concrete printing with various manufacturing constraints, *Additive Manuf.* 57 (2022), 102982, <https://doi.org/10.1016/j.addma.2022.102982>.